miR-215 regulates the homeostasis of small intestine

miR-215 は小腸の恒常性維持に重要な役割をはたす

Ksenia Sanchenkova

Department of Immune Regulation, Immunology Frontier Research Center, Graduate School of Frontier Biosciences, Osaka University, Osaka, Japan, 2021.06.

Summary

MicroRNAs are a class of non-coding short-chained RNAs, which control many functions of a cell by down-regulating their target genes. Recent works indicate that miRNAs play a role in the maintenance of a gut homeostasis. miR-215 was found to be highly expressed in the epithelial cells of the small intestine, however the involvement of miR-215 in gut immunity was until now unknown. Here, we show that miR-215 downregulates CXCL12, which leads to elevated recruitment of Th17 cells into small intestine, resulting in a strong inflammation. Mice lacking miR-215 showed increased number of Th17 cells in the lamina propria of the small intestine with the enhanced CXCL12 expression in the epithelial cells. The mutant mice further showed the high susceptibility to an inflammation induced by indomethacin. Our finding opens a promising perspective of targeting miR-215 to treat inflammatory conditions in small intestine.

Table of contents

Introduction

MicroRNAs (miRNAs) are small, non-coding RNAs, which are able to regulate gene expression both negatively and positively [1, 2, 3, 4, 5]. They originate from nucleus and genes, coding for miRNAs were thought to be unnecessary some time ago. In a form of a very long single-stranded RNA chain, which then undergoes self-pairing and finally gets the form of a hair-pin, miRNA is getting out from nucleus. The whole enzymatic machinery is then applied to the molecule to turn the hair-pin into a single-stranded short miRNA. This miRNA, being now a part of an Argonaut complex, will search for its complementary target messenger RNA (mRNA) to bind with it, forming again a double-stranded structure, which will be broken by Argonaut complex (appear as a kind of a "self-destruction" mechanism). Therefore, a protein will never be produced. That is a mechanism called "gene-silencing". All cells in a living organism possess the same genome. Yet, the diversity of different types of cells in organism is stunning: every tissue develops its own specific cell type, depending on the needs of each tissue. This is happening because it is no matter which genes are inside of a cell, but which of them are used and how efficiently – and that is the work of miRNAs – to control our gene expression in different tissues, dependently on the needs. Hence, the evolutionary role of miRNAs is hard to be over-estimated. This is exactly the example when small things are making big differences. It seems, that those little molecules can change the whole way of our genes' work. miRNAs are directing and fine-tuning the genes' expression in a similar way as a batonist is directing an orchestra: a perfect chemical orchestra of a living organism, by starting, ending and regulating milliards of biochemical reactions' cascades. Many factors can influence on miRNAs: basically, any potentially chemically reactive molecule can have an influence on that mechanism. Thus, by understanding the miRNAs' role and the mechanism of action, investigation of precisely targeted and directed medicines becomes possible, as well as more fine and elegant way of treatment of many diseases.

There are many works, indicating a big role of miRNAs in a gut homeostasis. It was demonstrated that miR-30, which is highly expressed in proliferating cells, rather than in differentiated cells, if being knockdown leads to reduction in proliferation, but increase in enterocyte differentiation [6]. Another microRNA miR-7 was shown to control epithelial cell adhesion and cell-cell interaction while migrating along the crypt-villus axis, by regulating the expression level of CD98 protein in the extracellular matrix [7, 8]. Several works demonstrated that miRNA-induced gene regulation has an impact on susceptibility of intestinal epithelial cells (IECs) to inflammation [9]. miR-200b, by regulating the level of cyclin D1, promotes proliferation in IECs. miR-200b is downregulated in inflammatory bowel disease (IBD) patients in dependence of severity of the illness [10]. Study of Liao's group pointed to the miR-146b regulating a transforming growth factor β (TGF-β), which dysregulation promotes uncontrolled growth and cell differentiation in the intestinal epithelium [11,12]. miRNAs are also shown to regulate gut microbiota, because miRNA molecules, derived from IECs, goblet and Paneth cells were found within intestinal contents [13]. The exosomal miRNAs were demonstrated to be released into the extracellular space [14]. These miRNAs were found to be differentially distributed through gastrointestinal (GI) tract, preferably in the area of ileal lumen. Liu demonstrated that a shift in gut microbiota is connected to reduction of luminal miRNAs and proposed that the host-produced miRNAs by entering gut bacteria can regulate their gene transcription programs [13]. It is still not clear about the precise mechanisms of miRNAs entering bacteria and manipulating their gene expression profiles, but the data demonstrate the powerful effect of the host-secreted miRNAs on bacterial growth and probably opens a way of manipulation of gut microbiota. There are evidences indicating that not only the host miRNAs are capable of inducing changes in microbiota, but vice-versa: gut bacteria regulate profile of the host miRNA [15, 16, 17]. It is well known that gut microbiota is able to mediate disease development through different mechanisms. But, it seems now

that many of those mechanisms involve miRNAs. Intestinal homeostasis can be altered by microbial metabolites, which induce miRNAs regulating the gene expression. Therefore, the ability of the host to change its microbiota through the host-secreted miRNAs, which affect bacterial growth and most likely their gene expression programs, are giving clear evidences to how important the role of miRNAs in intestinal homeostasis and cross-talk between host and microbiota can be. The further investigations in role of miRNAs in GI tract will help to understand the pathogenesis of many diseases, such as IBD, colitis and others and find the new miRNA targets for successful treatment of them.

Here we aim to study miRNAs, which are synthesized in gut epithelial cells and play a role in maintaining the gut homeostasis.

Materials and methods

Mice and cell lines

ICR and ICR-germ-free mice were purchased from CLEA Japan (Shizuoka, Japan). C57BL/6J mice were purchased from Japan SLC (Hamamatsu, Japan). Male mice were used for experiments. All animal experiments were conducted in accordance with guidelines of the Animal Care and Use Committee of Osaka University (Osaka, Japan).

Preparation of epithelial and lamina propria cells in the intestine

For isolation of intestinal epithelial cells and lamina propria cells, intestines were opened, washed to remove fecal content, shaken in HBSS containing 5 mM EDTA for 20 minutes at 37°C. Epithelial cells were collected from the suspension and the remaining tissue was cut into small pieces and incubated with RPMI 1640 containing 4% FBS, 1 mg/mL collagenase D (Roche, Indianapolis, IN), 0.5 mg/mL dispase (Invitrogen) and 40 μg/mL DNase I (Roche) for 20 minutes at 37°C in a shaking water bath. The digested tissues were washed with HBSS containing 5 mM EDTA and resuspended with 5 mL 40% Percoll (GE Healthcare, Buckinghamshire, UK), and then 80% Percoll was added to the bottom of tube to form the 80% (lower)/40% (upper) Percoll layers. After Percoll density gradient centrifugation, the lamina propria lymphocytes and granulocytes were collected at the Percoll gradient interface.

RNA-sequencing

Total RNA was extracted from cells with miRNeasy Mini kit (Qiagen, Hilden, Germany) according to the manufacturer's protocol. Full-length cDNA was generated using a SMART-Seq HT Kit (Takara Bio, Mountain View, CA) according to the manufacturer's instructions. An Illumina library was prepared using a Nextera DNA Library Preparation Kit (Illumina, San Diego, CA) according to SMARTer kit instructions. Sequencing was performed on an Illumina HiSeq 2500 sequencer

(Illumina) in the 75-base single-end mode. Illumina Casava 1.8.2 software was used for base calling. Sequenced reads were mapped to the mouse reference genome sequence (mm10) using TopHat v2.0.12 (Available: ccb.jhu.edu/software/tophat/) (Trapnell et al., 2014). Fragments per kilobase of exons per million mapped fragments (FPKMs) were calculated using Cufflinks v2.1.1 (Available: http://cole-trapnell-lab.github.io/cufflinks/) (Trapnell et al., 2013).

Quantitative RT-PCR analysis

Total RNA was purified with a RNeasy Mini Kit (Qiagen, Hilden, Germany) and reverse transcribed with ReverTra Ace qPCR RT Master Mix (Toyobo, Osaka, Japan). Quantitative RT–PCR was performed on a Step One Plus™ Real-Time PCR System (Applied Biosystems, Foster City, CA) using Power SYBR Green PCR Master Mix (Thermo Fisher Scientific, Waltham, MA). All values were normalized to the expression of *Gapdh*, which encodes glyceraldehyde-3-phosphate dehydrogenase; fold-differences in expression relative to *Gapdh* are shown. Amplification conditions were 95 °C (10 minutes) and 40 cycles of 95 °C (15 seconds) and 60 °C (60 seconds). The primer sets are as follows: *Gapdh* sense: 5'-CCTCGTCCCGTAGACAAAATG-3'; *Gapdh* antisense: 5'-TCTCCACTTTGCCACTGCAA-3'; *Cxcl12* sense: 5'-GCGCTCTGCATCAGTGAC-3'; *Cxcl12* antisense: 5'-TTTCAGATGCTTGACGTTGG-3'; *Cxcl14* sense: 5'-GTCACCACCAAGAGCATGTCCAG-3'; *Cxcl14* antisense: 5'-TCGTTCCAGGCATTGTACCACTTG-3'; *Cxcr4* sense: 5'-GTTGCCATGGAACCGATCA-3'; *Cxcr4* antisense: 5'-TGCCGACTATGCCAGTCAAGA-3'; *Il17* sense: 5'-CTCCAGAAGGCCCTCAGACTAC-3'; *Il17* antisense: 5'-AGCTTTCCCTCCGCATTGACACAG-3'.

Quantitation of miRNA expression

For detection of mature miR-215, 10 ng total RNA was reverse transcribed in vitro to cDNA using the TaqMan MicroRNA Reverse Transcription kit (Applied Biosystems, Foster City, CA USA) according to the manufacturer's instructions. miR-215 was assayed by TaqMan probe directed real-time PCR (Assay ID-001200; Reporter-FAM, Quencher-NFQ-MGB, Applied Biosystems, Foster City, CA, USA) using ABI 7500 Fast Real-Time PCR system (Applied Biosystems, Foster City, CA, USA). The following thermal cycling program was used for the analysis: 95°C for 10 minutes, 45 cycles at 95°C for 15 seconds, and 60°C for 1 minute. Each qPCR reaction was performed in triplicate. Expression levels of miRNAs were normalized to that of sno202.

Laser capture microdissection (LCM)

Small intestine tissues were excised and embedded in Optimum Cutting Temperature (OCT) compound (Sakura, Torrance, CA), The sections were cross-sectioned to 10 μm-thick slices using a cryostat (Leica CM1860, Leica Biosystems, Heidelberger, Germany) at -20°C onto PEN membrane glass slides and stored at -80°C. The slides were processed through a graded series of ethanol for fixation and dehydration, and stained with hematoxylin & eosin and alcian blue stains to identify enterocytes, Paneth cells and goblet cells respectively. After the slides were air-dried in a sterile environment, the laser capture microdissection was performed immediately by using a Leica LMD 7000 laser microdissection system (Leica). 10 μl of QIAzol (Qiagen) was pipetted into the lid of the cap prior to loading PCR tubes in the collection device of instrument. Microdissections were performed by drawing a circle using laser beam around the respective cells with the laser settings of: Power 25, Aperture 5, Speed 15 and Specimen balance 11. The cut sections were collected in the lid. Total RNA was

isolated immediately using the miRNeasy Micro Kit (Qiagen, Hilden, Germany). Around 1000 cell sections per biological replicate were collected.

miR-215-deficient mouse

Mice lacking miR-215 were generated in Dr. Takeda's laboratory (Graduate School of Medicine, Osaka University) and used for the experiments. Briefly, a targeting vector containing a neomycin resistance gene was used to generate miR-215-floxed mice. The targeting vector was constructed so that the genome encoding miR-215 was flanked by loxP sites. The targeting vector was electroporated into embryonic stem (ES) cells and selected by G418 (Nacalai Tesque, Kyoto, Japan). Clones with homologous recombination were identified by PCR and Southern blotting analysis and microinjected into blastocysts of C57BL/6 mice. Germ line transmission of the mutant allele was confirmed by Southern blotting. To generate systemic miR-215 deficient mice, heterozygous miR-215-floxed mice (*miR-215*$^{flox/+}$) were mated with CAG-Cre transgenic mice. Deletion of the floxed allele was confirmed by genomic PCR (WT: 450 bp; KO: 350 bp). 5'-TCTGGGTGGGCTCTTGGTTATCATTT-3' and 5'-GATTGAGCAGTCGGTGAGTGAGATGA-3' were used as PCR primers.

Gut permeability test

Mice were fasted for 4 hours and 4-kDa fluorescein isothiocyanate (FITC dextran) (Cat#FD4-250MG; Sigma-Aldrich, Steinheim, Germany) was administered orally (12 mg/mouse, 60 mg/mL in PBS). Blood was sampled 4 hours after the oral gavage. Serum was obtained after centrifugation at 3000 rpm for 5 minutes. Fluorescence was measured spectrophotometrically using SH-9000Lab Multigrading Micro Plate Reader (Corona Electric Co., Ltd, Ibaraki, Japan) in 96-well plates (excitation: 490 nm, emission: 520 nm). FITC dextran concentrations were calculated with the help of

standard concentrations prepared in PBS ranging from 0.06 to 6000 μg/mL of FITC dextran.

Flow cytometry

For immune cell subset isolation, purified lamina propria cells were sorted using flow cytometry (FACSAria, BD Biosciences, Franklin Lakes, NJ) after staining with the following fluorochrome-conjugated antibodies: fluorescein isothiocyanate (FITC)-conjugated anti-CD11b (Clone M1/70; Cat#101206; BioLegend, San Diego, CA) and anti-CD8a (Clone 53-6.7; Cat#100706; BioLegend), phycoerythrin (PE)-conjugated anti-IL10 (Clone JES5-16E3; Cat#505008; BioLegend), anti-Ly6G (Clone 1A8; Cat#551461; BD Biosciences) and anti-B220 (CD45RB) (Clone C363-16A; Cat#103308; BioLegend), allophycocyanin (APC)-conjugated anti-IL17A (Clone TC11-18H10.1; Cat#506916; BioLegend), anti-CD11c (Clone N418; Cat#20-0114-U100; Tonbo bioscience, San Diego, CA) and anti-CD4 (Clone GK1.5; Cat#100412; BioLegend), phycoerythrin/cyanin 7 (PE/Cy7)-conjugated anti-IFNγ (Clone XMG1.2; Cat#505825; BioLegend), and pacific blue-conjugated anti-CD4 (Clone GK1.5; Cat#100428; BioLegend) and anti-CD45 (Clone 30-F11; Cat#103126; BioLegend). Myeloid cell populations were gated as $CD45^+$ $CD11b^+$ $CD11c^-$ $Ly6G^+$ (Neutrophil) and $CD45^+$ $CD11b^-$ $CD11c^+$ (conventional dendritic cell (cDC)). Lymphocyte populations were gated as $CD45^+$ $CD4^+$ $CD8^-$ $B220^-$ ($CD4^+$ T cell), $CD45^+$ $CD4^-$ $CD8^+$ $B220^-$ ($CD8^+$ T cell) and $CD45^+$ $CD4^-$ $CD8^-$ $B220^+$ (B cell). $CD4^+$ T cell populations were gated as $CD4^+$ $IFN\gamma^+$ $IL10^-$ $IL17A^-$ (Th1), $CD4^+$ $IFN\gamma^-$ $IL10^+$ $IL17A^-$ (Th2) and $CD4^+$ $IFN\gamma^-$ $IL10^-$ $IL17A^+$ (Th17).

Indomethacin-induced intestinal inflammation

Ileitis was induced by oral administration of 3 or 6.25 mg/kg/day of indomethacin (Cat#093-02473; Fujifilm Wako Pure Chemical Corporation, Osaka, Japan) (0.5 mg/mL

in 0.1 M $NaHCO_3$) for 5 days. Body weight was evaluated daily and mice were sacrificed at day 7 and length of small intestine was measured. For histological analysis, small intestinal specimens were prepared by a Swiss roll method and fixed with 4% paraformaldehyde phosphate buffer solution (Wako Pure Chemical Industries, Osaka, Japan) and embedded in paraffin. Sections were stained with hematoxylin and eosin and analyzed with a BZ-9000 microscope system (Keyence Corporation, Osaka, Japan).

Statistical analysis

All quantitative data that has been collected from experiments is expressed as mean ± s.d. as indicated in the figure legends. Statistical analyses were performed with the two-tailed unpaired Student's *t* test. The log-rank test was used for mice survival. Analyses were conducted by using GraphPad Prism 8 software (GraphPad software, San Diego, CA). *P* values of less than 0.05 were considered statistically significant.

Results

miR-215 is highly expressed in the small intestinal enterocytes

First of all, I aimed to find out which miRNAs are highly expressed in intestinal epithelial cells (IECs), therefore I performed RNA-sequencing of epithelial cells (ECs) of small intestine (SI) and large intestine (LI) of mice, housed in specific-pathogen free (SPF) and germ-free (GF) conditions (Fig.1A). Several miRNAs were found to be highly and specifically expressed in SI and LI of SPF and GF mice: miR-194, miR-192, and miR-215. Expression of these miRNAs was significantly higher in SI than in LI. In addition, expression of three miRNAs was equally observed in SPF and GF mice, indicating that these miRNAs are expressed in a microbiota-independent manner. Among these miRNAs, miR-215 is highly expressed in SI, but only slightly expressed in LI. Therefore, I decided to analyze the role of miR-215 in SI. I analyzed in which part of the intestine miR-215 is expressed. Therefore, I isolated small intestinal ECs from proximal, middle and distal compartments of SI, ECs of LI, and lamina propria cells (LPCs) from SI and LI, and performed Q-PCR (Fig.1B). I found that expression of miR-215 is higher in proximal and middle compartments of SI. To find out whether or not miR-215 expression depends on microbiota, I compared the expression of miR-215 in SPF and GF mice by isolating ECs and LPCs of SI and performed Q-PCR of mRNA encoding for miR-215 (Fig.1C). I found that miR-215 is equally expressed in SPF and GF mice, indicating that miR-215 expression is independent on microbiota. Then, I tried to find which types of cells in SI mostly expresses miR-215. For that purpose, small intestinal epithelial cell subsets: goblet cells (GCs), enterocytes (ENTs) and Paneth cells (PCs) were isolated from SI by laser capture microdissection. Q-PCR was performed to measure the levels of mRNA encoding for miR-215 (Fig.1D). Small intestinal ENTs expressed the highest level of miR-215. Thus, I found that miR-215 is highly expressed in ENTs of the proximal compartment of SI independently of microbiota.

miR-215 deficiency increases $CD4^+$ effector T cells in small intestinal lamina propria

Next, I decided to analyze the function of miR-215. To assess the role of miR-215 in gut immunity, miR-215-deficient (KO) mice were generated by gene targeting. To confirm the phenotype, genotyping of tail-DNA of wild-type (WT) and miR-215 KO mice by PCR was performed (Fig. 2A). The absence of miR-215 expression was confirmed by Q-PCR of mRNA encoding for miR-215 of ECs of SI and LI of WT and KO animals (Fig. 2B). Thus, the successful generation of a KO mouse model was confirmed. Next, I analyzed the phenotype of miR-215 KO mice. First, I checked developing ECs. For that purpose, hematoxylin & eosin staining of small intestinal tissues of WT and *m*iR-215 KO animals was performed (Fig. 2C). The result demonstrated no differences between WT and KO animals, indicating that there was no impairment in the development of small intestinal ECs in miR-215 KO mice. Next, I analyzed if miR-215 deficiency affects barrier function of ECs. Mice were fasted for 4 hours and fluorescein isothiocyanate-labeled dextran (FITC-dextran) was administered orally and serum concentration of FITC-dextran was measured (Fig. 2D). No difference in serum FITC-dextran concentration was found between WT and miR-215 KO animals, indicating that the barrier function was not anyhow affected upon depletion of miR-215. Then, I aimed to analyze whether miR-215 deficiency affects the status of mucosal immune system. I analyzed the number of $CD4^+$ T cells in lamina propria of SI and LI of WT and miR-215 KO animals by performing flow cytometric analysis of total $CD4^+$ T cells (Fig. 2E). The number of $CD4^+$ T cells was increased in SI of miR-215 KO animals. Then, I analyzed what kinds of $CD4^+$ T cells was increased in miR-215 KO animals by performing flow cytometric analysis of $CD4^+$ T cell subsets from WT and miR-215 KO small and large intestinal lamina propria (Fig. 2F). Th1 cells producing IFN-γ and Th17 cells producing IL-17 were significantly increased in the

small intestine of miR-215 KO mice. Thus, the number of Th1 and Th17 cells were increased in the SI of miR-215 KO mice in healthy condition.

Establishment of a mouse model of small intestinal inflammation

Because I found that the number of Th1 and Th17 cells was increased in miR-215 KO mice, I then aimed to analyze the consequence of the increased number of Th1 and Th17 cells in the maintenance of small intestinal homeostasis. Indomethacin (IND) is known as a non-steroidal anti-inflammatory drug, which has successfully been applied in humans as pain killer and for reduction of fever, swelling and other inflammation signs. However, IND is well known to induce small intestinal inflammation in rodents. It was also shown that IND and other non-steroidal anti-inflammatory drugs (NSAIDs) are able to elevate the infiltration of $CD4^+$ T-helper cells [18]. Thus, I tried to establish a protocol to induce small intestinal inflammation by IND treatment in mice. I demonstrated that oral administration of 6.25 mg/kg/day of IND in drinking water showed the most acceptable results in mice. Next, WT animals were administrated with 6.25 mg/kg of IND in drinking water for 6 days, while control group animals were receiving drinking water. The changes in body weight were recorded every day during the course (Fig. 3A). At day six of experiment, all mice were sacrificed and their SIs were isolated (Fig. 3B). IND-treated WT animals showed severe body weight loss and shorter length of SI in comparison with mice receiving only water without IND. Next, I analyzed histopathological changes in IND-treated animals. For that purpose, hematoxylin & eosin staining of small intestinal tissues of WT animals receiving IND and pure water was performed (Fig.3C). Disruption in epithelial layers, ulcerations and infiltration of inflammatory cells in small intestinal tissues were evident in WT mice treated with IND, while no signs of inflammation were seen in WT mice receiving water with no IND. Thus, I successfully established the protocol to induce small intestinal inflammation by IND.

In the next experiment, I analyzed immune cell population in this IND-induced small intestinal inflammation model. First, I analyzed $CD45^+$ cell subsets: neutrophils, $CD11c^+$ cDCs, $CD4^+$ T cells, $CD8^+$ T cells and B cells by flow cytometry (Fig. 3D). I found that the number of neutrophils and $CD4^+$ T cells and $CD8^+$ T cells was increased in IND-induced inflammation, which was consistent with previous data [18]. Then, I analyzed which types of $CD4^+$ T cells was increased in WT animals under IND-induced ileitis. I performed flow cytometric analysis of intracellularly-stained $CD4^+$ T cells harvested from the small intestinal lamina propria of WT mice that were treated with IND and control group (Fig. 3E). The number of Th17 cells producing IL-17 was significantly increased in IND-treated WT mice. Thus, I demonstrated that small intestinal inflammation induced by oral administration of IND leads to increase in the number of neutrophils, $CD8^+$ T cells and Th17 cells. Since the number of Th17 cells was increased in IND-treated animals, I then analyzed expression of chemokines in IECs, which can mediate the recruitment of Th17 cells. Small intestinal ECs of WT mice treated with IND and pure water were isolated, and analyzed by Q-PCR of mRNA encoding *Cxcl12* and *Cxcl14* (Fig.3F). *Cxcl12* mRNA expression was found to be markedly increased in IECs of WT mice after IND-treatment. Thus, I successfully established a protocol to induce small intestinal inflammation, in which IND induced expression of *Cxcl12* in the IECs and increased the number of Th17 cells in the small intestinal lamina propria.

High sensitivity to IND-induced inflammation in miR-215 KO mice

Since I successfully established the protocol for IND-induced small intestinal inflammation, I then tried to analyze the effect of miR-215 deficiency in IND-induced ileitis. WT and miR-215 KO mice were treated with either drinking water containing or without IND for 6 days. The survival rate and body weight loss were recorded every day during the 6 days course (Fig. 4A and B). miR-215 KO animals exhibited increased

mortality by administration of 6.25 mg/kg/day of IND. Even with decreased dose of IND (3 mg/kg/day for 5 days), severe body weight loss was induced in miR-215 KO animals . On day 6 of the experiment, all mice treated with 3mg/kg/day of IND were sacrificed and their SIs were analyzed (Fig. 4C). The length of SIs of miR-215 KO animals was shorter than SI length in WT animals. To assess the severity of intestinal inflammation in miR-215 KO and WT mice, I performed hematoxylin & eosin staining of small intestinal tissues of miR-215 KO and WT animals (Fig. 4D). The severity of intestinal inflammation was much higher in miR-215 KO mice as evidenced by rupture in epithelial layers, ulcerations and influx of inflammatory cells. Next, I compared immune cell population in *miR*-215 KO and WT mice after IND-induced small intestinal inflammation. First, I analyzed $CD45^+$ cell subsets: neutrophils, whole T cells and $CD4^+$ T cells by flow cytometry (Fig.4E). I found that in miR-215 KO mice, the number of neutrophils, $CD4^+$ T cells and whole T cells was increased after IND-induced inflammation than in WT mice. Next, I performed Q-PCR of mRNA encoding for *Il17* of $CD4^+$ T cells (Fig.4F). Expression of *Il17* were higher in $CD4^+$ T cells of miR-215 KO mice, indicating that the number of IL-17-producing Th17 cells were increased in IND-treated miR-215 KO mice. To check expression of chemokines in IECs, small intestinal ECs of miR-215 KO and WT mice treated with IND were isolated and analyzed by Q-PCR of mRNA encoding *Cxcl12* and *Cxcl14* (Fig. 4G). *Cxcl12* mRNA expression was found to be higher in IECs of IND-treated miR-215 KO mice than in IND-treated WT mice. These findings suggest that the elevated number of IL-17-producing $CD4^+$ T cells in miR-215 KO animals is due to aberrant expression of CXCL12 chemokine in epithelial cells.

Discussion

The overall history of miRNAs exploration counts only 20 years [19, 20, 21, 22, 23]. When they were first discovered in early 1990's, they were not even classified as a separate class of RNA molecules. Now however, since more and more emerging data demonstrate important functions of miRNA in the organism, a truly gigantic role of a small molecule in maintaining the right balance in each cell is now not fully, but understood. Yet, many unknown functions are still to be discovered. Recent works on miRNAs open their entirely new fascinating regulatory functions in almost all tissues of organism and elucidate miRNAs as developmental regulators [19, 20, 21, 23, 24, 25, 26, 27, 28, 29, 30]. The fact, that the level of expression of a single miRNA can change the whole program of a cell opens entirely new approaches in medicine: targeting miRNAs and controlling their expression.

miR-215 is not well investigated yet and not so much is known about its functions in human body. Some works clearly demonstrate the benefits of miR-215 overexpression in anti-cancer therapies [31, 32], while other works vice-versa show that upregulated miR-215 levels were found in several types of malignancies [33, 34]. Here, the role of miR-215 in the maintenance of gut homeostasis is shown for the first time. We demonstrated that downregulation of miR-215 in IECs elevates the levels of CXCL12 - a chemoattractant for Th17 cells, which leads to higher recruitment of inflammatory cells and exacerbates SI inflammation.

The question still remaining is how miR-215 regulates CXCL12. In this study I focused only on CXCL12, because I used IND-induced SI inflammation mediated by Th17 cells. In the future, I will also have to analyze whether miR-215 directly or indirectly regulates the *Cxcl12* gene. For this analysis I will be able to perform a luciferase assay. I will also have to analyze genes, which are aberrantly expressed in IECs of miR-215 KO animals by RNA-sequencing.

In this study, I focused on IND-induced SI inflammation. But miR-215 is supposed to regulate several genes in addition to *Cxcl12*. Therefore, it is possible that miR-215 in IEC modulates other aspects of activities that control gut homeostasis. In the future, I would like to analyze additional functions of miR-215.

In this work, I found that miR-215 regulates the homeostasis of the SI. Targeting miR-215 would be a promising approach for a treatment of small intestinal inflammation.

References

1. David Baltimore, Mark P Boldin, Ryan M O'Connell, Dinesh S Rao, Konstantin D Taganov, 2008. MicroRNAs: new regulators of immune cell development and function. *Nat. Immunol.* **9 (8)**: 839-45.
2. Antoaneta Belcheva, 2017. MicroRNAs at the epicenter of intestinal homeostasis. *Bioessays* 39, 3, 1600200.
3. Rajesha Rupaimoole, Frank J. Slack, 2017. MicroRNA therapeutics: towards a new era for the management of cancer and other diseases. *Nat. Rev. Drug Discovery* **16**, 203-222.
4. Jean-Malo Couzigou, Dominique Lauressergues, Olivier Andre, Caroline Gutjahr, Bruno Guillotin, Guillaume Be´ card, Jean-Philippe Combier, 2017. Positive Gene Regulation by a Natural Protective miRNA Enables Arbuscular Mycorrhizal Symbiosis. *Cell Host & Microbe* **21**, 106–112.
5. Peng Xu, Qian Wu, Jian Yu, Yongsheng Rao, Zheng Kou, Gang Fang, Xiaolong Shi, Wenbin Liu, Henry Han, 2020. A systematic way to infer the regulation relations of miRNAs on target genes and critical miRNAs in cancers. *Front. Genet.* **11**: 278.
6. Peck BC, Sincavage J, Feinstein S, Mah AT, et al. 2016. MiR-30 family controls proliferation and differentiation of intestinal epithelial cell models by directing a broad gene expression program that includes SOX9 and the ubiquitin ligase pathway. *J Biol Chem* **291**: 15975– 84.
7. Nguyen HT, Dalmasso G, Yan Y, Laroui H, et al. 2010. MicroRNA-7 modulates CD98 expression during intestinal epithelial cell differentiation. *J Biol Chem* **285**: 1479– 89.

8. Yan Y, Vasudevan S, Nguyen HT, Merlin D. 2008. Intestinal epithelial CD98: an oligomeric and multifunctional protein. *Biochim Biophys Acta* **1780**: 1087–92.
9. Lee J, Park EJ, Yuki Y, Ahmad S, et al. 2015. Profiles of microRNA networks in intestinal epithelial cells in a mouse model of colitis. *Sci Rep* **5**: 18174.
10. Chen Y, Xiao Y, Ge W, Zhou K, et al. 2013. miR-200b inhibits TGF-beta1-induced epithelial-mesenchymal transition and promotes growth of intestinal epithelial cells. *Cell Death Dis* **4**: e541.
11. Liao Y, Zhang M, Lonnerdal B. 2013. Growth factor TGF-beta induces intestinal epithelial cell (IEC-6) differentiation: miR-146b as a regulatory component in the negative feedback loop. *Genes Nutr* **8**: 69– 78.
12. Wharton K, Derynck R. 2009. TGFbeta family signaling: novel insights in development and disease. *Development* **136**: 3691– 7.
13. Liu S, da Cunha AP, Rezende RM, Cialic R, et al. 2016. The host shapes the gut microbiota via fecal microRNA. *Cell Host Microbe* **19**: 32– 43.
14. Sato-Kuwabara Y, Melo SA, Soares FA, Calin GA. 2015. The fusion of two worlds: non-coding RNAs and extracellular vesicles-diagnostic and therapeutic implications (Review). *Int J Oncol* **46**: 17– 27.
15. Larsson E, Tremaroli V, Lee YS, Koren O, et al. 2012. Analysis of gut microbial regulation of host gene expression along the length of the gut and regulation of gut microbial ecology through MyD88. *Gut* **61**: 1124– 31.
16. Camp JG, Frank CL, Lickwar CR, Guturu H, et al. 2014. Microbiota modulate transcription in the intestinal epithelium without remodeling the accessible chromatin landscape. *Genome Res* **24**: 1504– 16.

17. Dalmasso G, Nguyen HT, Yan Y, Laroui H, et al. 2011. Microbiota modulate host gene expression via microRNAs. *PLoS ONE* **6**: e19293.

18. Christina Loennroth, Marianne Andersson, Annette Arvidsson, Svante Nordgren, Hans Brevinge, Kristina Lagerstedt and Kent Lundholm, 2008. Preoperative treatment with a non-steroidal anti-inflammatory drug (NSAID) increases tumor tissue infiltration of seemingly activated immune cells in colorectal cancer. *Cancer Immunity* **8**: 5.

19. Bartel, D. P. MicroRNAs: genomics, biogenesis, mechanism, and function. *Cell* **116**, 281–297 (2004).

20. Lee, R. C., Feinbaum, R. L. & Ambros, V. The *C. elegans* heterochronic gene *lin-4* encodes small RNAs with antisense complementarity to *lin-14*. *Cell* **75**, 843–854 (1993).

21. Reinhart, B. J. et al. The 21-nucleotide *let-7* RNA regulates developmental timing in *Caenorhabditis elegans. Nature* **403**, 901–906 (2000).

22. Pasquinelli, A. E. et al. Conservation of the sequence and temporal expression of *let-7* heterochronic regulatory RNA. *Nature* **408**, 86–89 (2000).

23. Esteller, M. Non-coding RNAs in human disease. *Nat. Rev. Genet.* **12**, 861–874 (2011).

24. Coussens, L. M. & Werb, Z. Inflammation and cancer. *Nature* **420**, 860–867 (2002).

25. Roush, S. & Slack, F. J. The *let-7* family of microRNAs. *Trends Cell Biol.* **18**, 505–516 (2008).

26. Iorio, M. V. & Croce, C. M. MicroRNA dysregulation in cancer: diagnostics, monitoring and therapeutics. A comprehensive review. *EMBO Mol. Med.* **4**, 143–159 (2012).
27. Tili, E., Michaille, J. J. & Croce, C. M. MicroRNAs play a central role in molecular dysfunctions linking inflammation with cancer. *Immunol. Rev.* **253**, 167–184 (2013).
28. Rupaimoole, R., Calin, G. A., Lopez-Berestein, G. & Sood, A. K. miRNA deregulation in cancer cells and the tumor microenvironment. *Cancer Discov.* **6**, 235–246 (2016).
29. Gurha, P. MicroRNAs in cardiovascular disease. *Curr. Opin. Cardiol.* **31**, 249–254 (2016).
30. Worringer, K. A. et al. The let-7/LIN-41 pathway regulates reprogramming to human induced pluripotent stem cells by controlling expression of prodifferentiation genes. *Cell Stem Cell* **14**, 40–52 (2014).
31. Jana Merhautova, Tana Machackova, Vychytilova-Faltejskova et al 2017. MiR-215-5p is a tumor suppressor in colorectal cancer targeting EGFR ligand epiregulin and its transcriptional inducer HOXB9. Oncogenesis 6:399.
32. Shahzad MMK, Felder M, Ludwig K, Van Galder HR, Anderson ML, Kim J, et al. (2018) Trans10,cis12 conjugated linoleic acid inhibits proliferation and migrationof ovarian cancer cells by inducing ER stress, autophagy, and modulation of Src. PLoSONE 13(1): e0189524.

33. Shanthi Sabarimurugan, Sunil Krishnan , Rama Jayaraj. 2020. Prognostic Value of MicroRNAs in Stage II Colorectal Cancer Patients: A Systematic Review and Meta-Analysis. Molecular Diagnosis & Therapy (2020) 24:15–30.

34. Xiaodun Li, Sam Kleeman, Sally B.Coburn, 2018. Selection and Application of Tissue microRNAs for Nonendoscopic Diagnosis of Barrett's Esophagus. *Gastroenterology* **155**: 771-783.

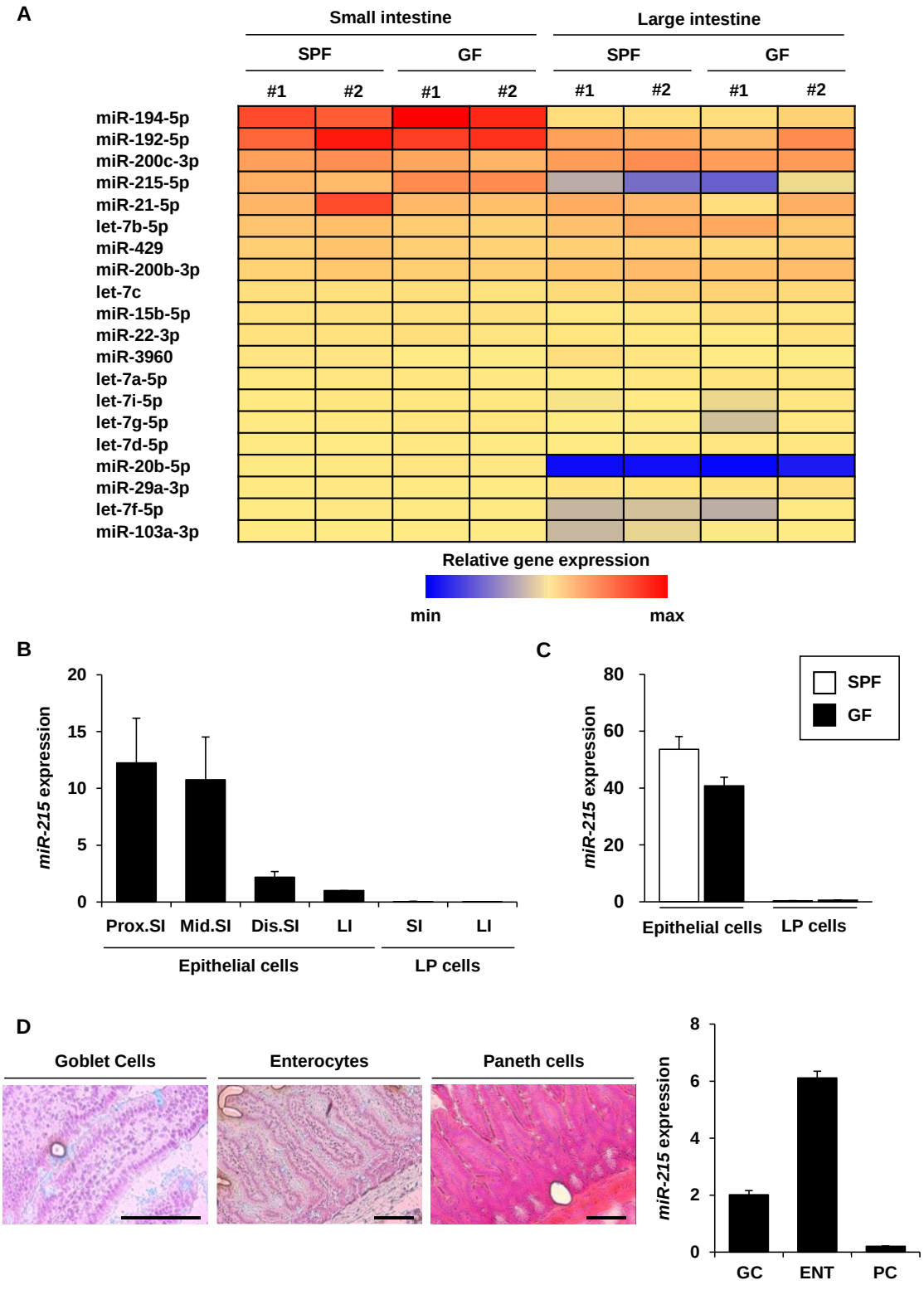
A
Small intestine
Large intestine
SPF
GF
SPF
GF
#1
#2
#1
#2
#1
#2
#1
#2
miR-194-5p
miR-192-5p
miR-200c-3p
miR-215-5p
miR-21-5p
let-7b-5p
miR-429
miR-200b-3p
let-7c
miR-15b-5p
miR-22-3p
miR-3960
let-7a-5p
let-7i-5p
let-7g-5p
let-7d-5p
miR-20b-5p
miR-29a-3p
let-7f-5p
miR-103a-3p
Relative gene expression
min
max
B
miR-215 expression
20
15
10
5
0
Prox.SI
Mid.SI
Dis.SI
LI
SI
LI
Epithelial cells
LP cells
C
miR-215 expression
80
60
40
20
0
SPF
GF
Epithelial cells
LP cells
D
Goblet Cells
Enterocytes
Paneth cells
miR-215 expression
8
6
4
2
0
GC
ENT
PC

Figure 1. miR-215 is highly expressed in the small intestinal enterocytes.

(A) RNA-seq heat map of duplicate samples of whole cell suspension harvested from small or large intestine of specific-pathogen-free (SPF) and germ-free (GF) mice. Color-codes indicate processed signals.

(B-D) Quantitative RT-PCR of mRNA encoding miR-215 in epithelial cells and lamina propria cells of the small and large intestine (B), epithelial cells and lamina propria cells harvested from small intestine of SPF and GF mice (C), small intestinal epithelial cell subsets (goblet cells (GC), enterocytes (ENT), and Paneth cells (PC)) collected by laser capture microdissection (D), normalized to miR-202 expression.

All data shown are representative of at least two independent experiments. Data are presented as mean ± s.d. (n = 2-4 per group).

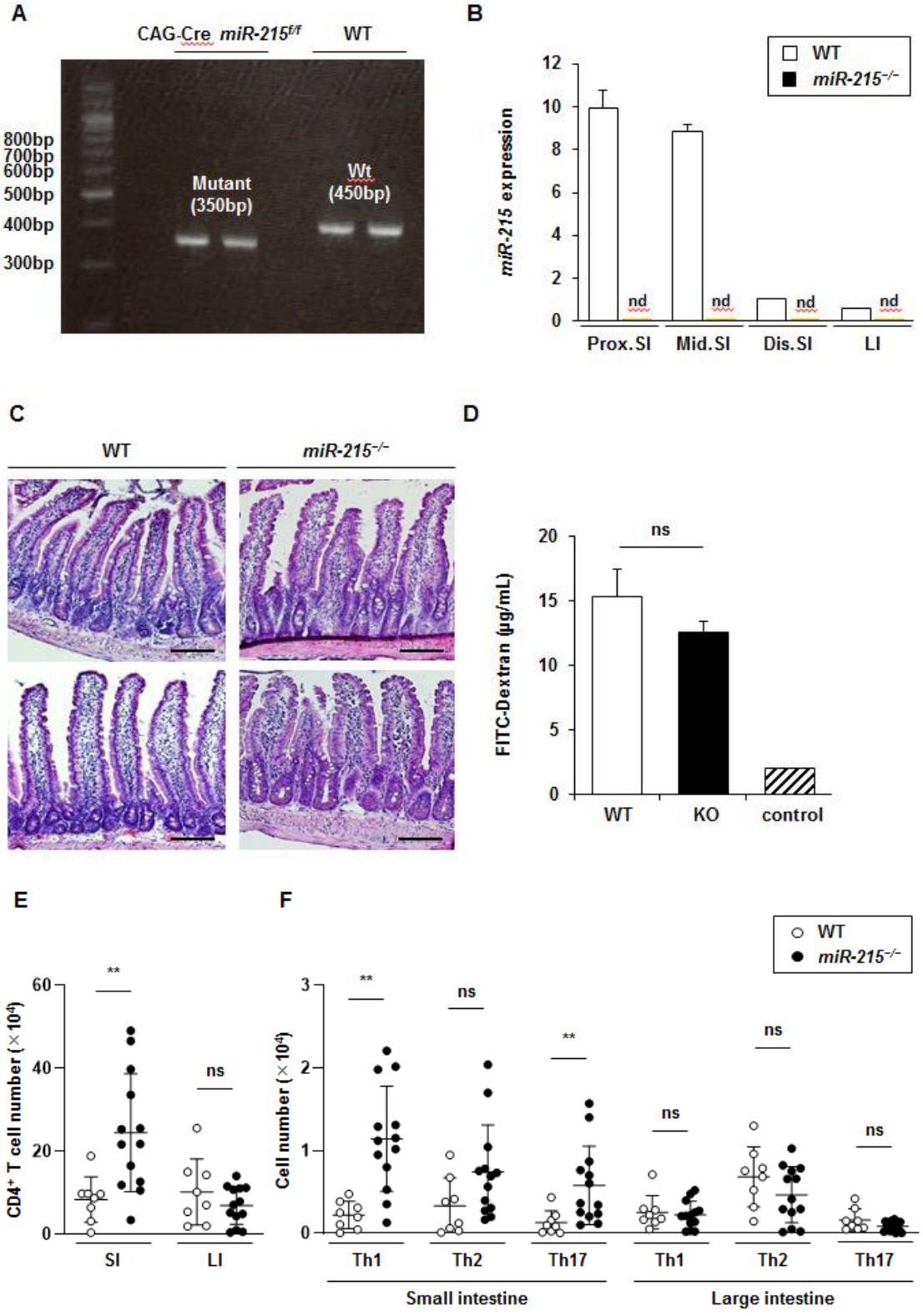
A
CAG-Cre miR-215f/f
WT
800bp
700bp
600bp
500bp
400bp
300bp
Mutant (350bp)
Wt (450bp)
B
WT
miR-215−/−
miR-215 expression
12
10
8
6
4
2
0
nd
Prox.SI
Mid.SI
Dis.SI
LI
C
WT
miR-215−/−
D
FITC-Dextran (μg/mL)
20
15
10
5
0
ns
WT
KO
control
E
CD4+ T cell number (×10⁴)
60
40
20
0
**
ns
SI
LI
F
WT
miR-215−/−
Cell number (×10⁴)
3
2
1
0
**
ns
**
ns
ns
ns
Th1
Th2
Th17
Th1
Th2
Th17
Small intestine
Large intestine

Figure 2. miR-215 deficiency increases CD4$^+$ effector T cells in healthy-state small intestinal lamina propria.

(A) PCR genotyping of wild type (WT) and CAG-Cre *miR-215$^{f/f}$* mice.

(B) Relative expression of miR-215 in epithelial and lamina propria cells of the proximal (Prox.), middle (Mid.) and distal (Dis.) small intestine (SI) and large intestine (LI) of WT and miR-215-deficient mice, normalized to miR-202 expression. nd, not detected.

(C) H&E staining of small intestinal tissues of healthy-state WT and miR-215-deficient mice. Scale bars, 100 μm.

(D) Intestinal permeability of WT and miR-215-deficient mice determined by serum FITC-dextran concentration, compared to control mice without dextran administration.

(E and F) Flow cytometric analysis of total CD4$^+$ T cells (E) and CD4$^+$ T cell subsets (F) harvested from WT and miR-215-deficient small and large intestinal lamina propria.

All data shown are representative of at least two independent experiments. Data are presented as mean ± s.d. (n = 4-13 per group). $^{**}p < 0.01$, ns, not significant.

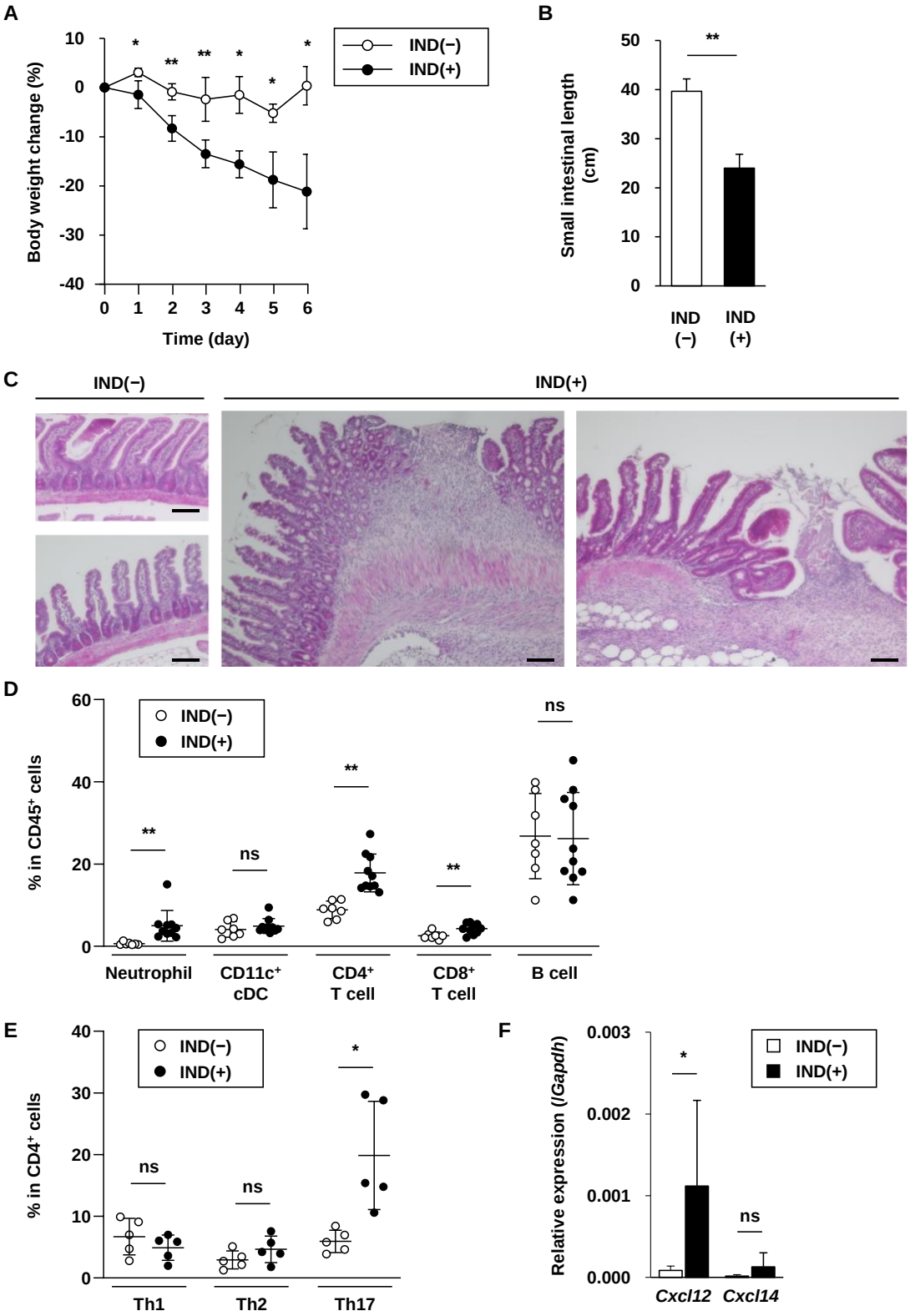
A
Body weight change (%)
Time (day)
IND(−)
IND(+)
B
Small intestinal length (cm)
IND (−)
IND (+)
C
IND(−)
IND(+)
D
% in CD45⁺ cells
Neutrophil
CD11c⁺ cDC
CD4⁺ T cell
CD8⁺ T cell
B cell
ns
E
% in CD4⁺ cells
Th1
Th2
Th17
F
Relative expression (/Gapdh)
Cxcl12
Cxcl14

Figure 3. Th17-dominant $CD4^+$ T cell differentiation is induced in the indomethacin-treated small intestine.

(A) Percentage of weight change of WT mice after oral administration of 6.25 mg/kg/day of indomethacin (IND(+); n = 4) or 0.1M $NaHCO_3$ (IND(−); n = 3).

(B and C) Small intestinal length (B), and H&E staining of small intestinal tissues (C) of WT mice with or without oral indomethacin administration.

(D and E) Flow cytometric analysis of immune cell subsets (D) and $CD4^+$ T cell subsets (E) harvested from small intestinal lamina propria of WT mice with or without oral indomethacin administration.

(F) Quantitative RT-PCR of mRNA encoding *Cxcl12* and *Cxcl14* in epithelial cells harvested from small intestine of WT mice with or without oral indomethacin administration, normalized to *Gapdh* expression.

All data shown are representative of at least two independent experiments. Data are presented as mean ± s.d. (n = 3-10 per group). *$p < 0.05$, **$p < 0.01$, ns, not significant.

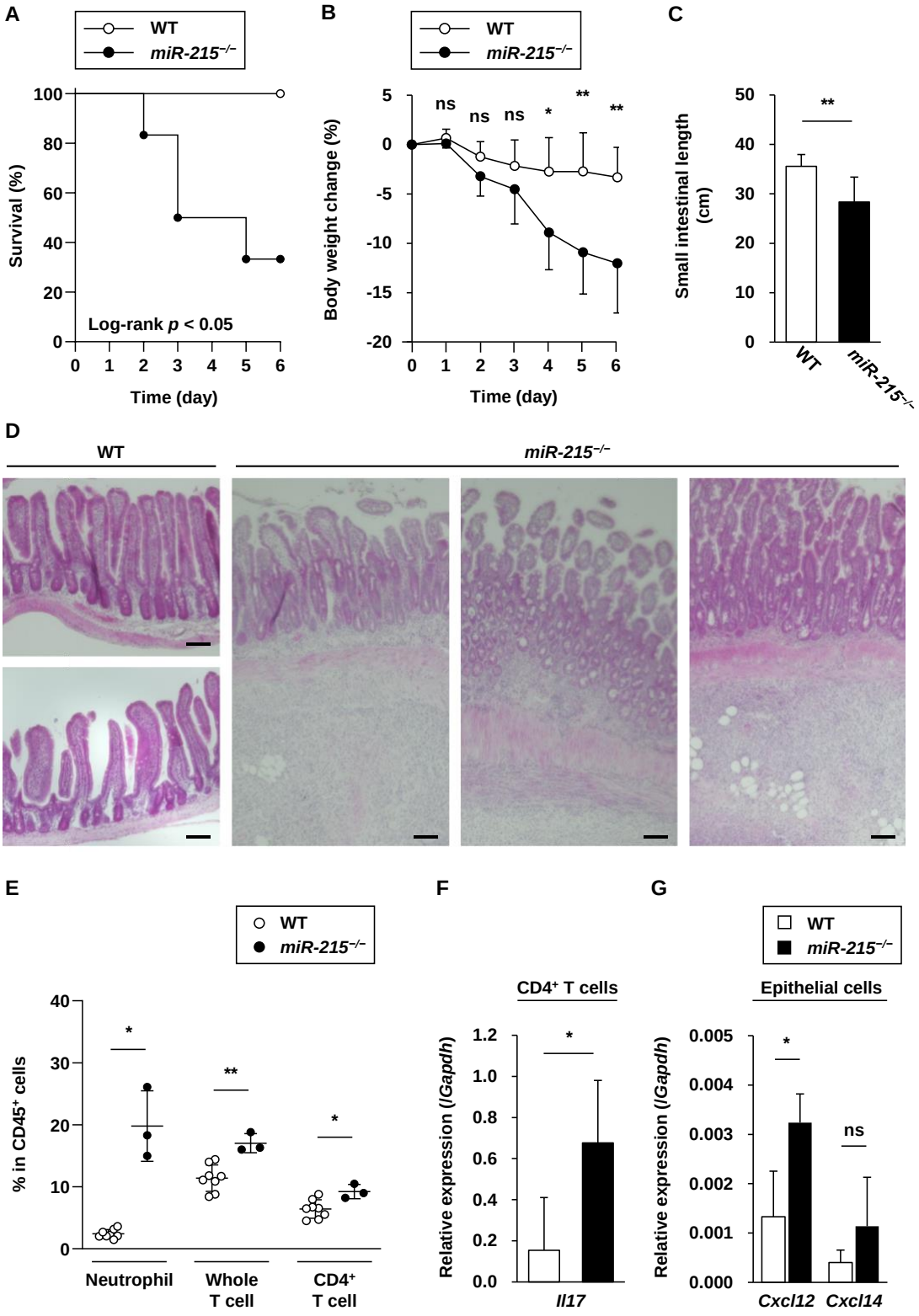
A
WT
miR-215−/−
Survival (%)
Log-rank p < 0.05
Time (day)
B
Body weight change (%)
ns
ns
ns
*
**
**
Time (day)
C
Small intestinal length (cm)
**
WT
miR-215−/−
D
WT
miR-215−/−
E
% in CD45+ cells
Neutrophil
Whole T cell
CD4+ T cell
F
CD4+ T cells
Relative expression (/Gapdh)
Il17
G
Epithelial cells
Relative expression (/Gapdh)
ns
Cxcl12
Cxcl14

Figure 4. miR-215 deficiency exacerbates ileal inflammation under low-dose indomethacin treatment.

(A) Survival rates of WT (n = 6) and miR-215-deficient (n = 6) mice after oral administration of 6.25 mg/kg/day of indomethacin. Data are pooled from two independent experiments. The log-rank test was used for survival analysis.

(B) Percentage of weight change of WT (n = 10) and miR-215-deficient (n = 6) mice after oral administration of 3 mg/kg/day of indomethacin.

(C and D) Small intestinal length (B), and H&E staining of small intestinal tissues (C) of WT and miR-215-deficient mice under oral indomethacin administration.

(E) Flow cytometric analysis of immune cell subsets harvested from small intestinal lamina propria of WT and miR-215-deficient mice under oral indomethacin administration.

(F and G) Quantitative RT-PCR of mRNA encoding *Il17* in lamina propria $CD4^+$ T cells (F), *Cxcl12* and *Cxcl14* in epithelial cells (G) harvested from small intestine of WT and miR-215-deficient mice under oral indomethacin administration, normalized to *Gapdh* expression.

All data shown are representative of at least two independent experiments. Data are presented as mean ± s.d. (n = 3-10 per group). *$p < 0.05$, **$p < 0.01$, ns, not significant.